Measurement Report: An Exploratory Study of Fluorescence and CCN Activity of Urban Aerosols in San Juan, Puerto Rico

Bighnaraj Sarangi [1*], Darrel Baumgardner[3], Benjamin Bolaños-Rosero[4] and Olga L. Mayol-Bracero[1, 2]

[1]Department of Environmental Sciences, University of Puerto Rico - Río Piedras Campus, San Juan, Puerto Rico, USA

[2] Now at Environment and Climate Sciences Department, Brookhaven National Laboratory, Upton, New York, USA

[3] Droplet Measurement Technologies LLC, Longmont, Colorado, USA

[4]Department of Microbiology, School of Medicine, University of Puerto Rico - Medical Sciences Campus, San Juan, Puerto Rico, USA

(*Correspondence: bighnarajsarangi1986@gmail.com)

Abstract

Many atmospheric aerosols are cloud condensation nuclei (CCN), capable of activating as cloud droplets when the relative humidity exceeds 100%. Some primary biological aerosol particles (PBAP), such as plant spores, pollen, or bacteria, have been identified as such CCN. Urban environments are a source of these bioaerosols, those that are naturally produced by the local flora, or are transported from surrounding regions, and others that are a result of human activities. In the latter case, open sewage, uncovered garbage, mold or other products of such activities can be a source of PBAPs. There have been relatively few studies, especially in the tropics, where PBAPs and CCN have been simultaneously studied to establish a causal link between the two. The metropolis of San Juan, Puerto Rico is one such urban area with a population of 2,448,000 people (as of 2020). To better understand the fluorescent characteristics and cloud forming efficiency of aerosols in this region, measurements with a

Wideband Integrated Bioaerosol Spectrometer (WIBS), a condensation nuclei (CN) counter, and a CCN spectrometer were made at the University of Puerto Rico – Rio Piedras Campus. Results show that the CCN/CN activation ratio and the fraction of fluorescing aerosol particles (FAP) have repetitive daily trends when the FAP fraction is positively correlated with relative humidity and negatively correlated with wind speed, consistent with previous studies of fungi spores collected on substrates.

The results from this pilot study highlight the capabilities of ultraviolet-induced fluorescence (UV-IF) measurements for characterizing the properties of FAP as they relate to the daily evolution of PBAPs. The use of multiple excitation and emission wavelengths, along with shape detection, allows the differentiation of different PBAP types. These measurements, evaluated with respect to previous, substrate-based analysis of the local fungal and pollen spores, have established a preliminary database of measurements that future, longer term studies will build upon.

1 Introduction:

The formation and evolution of clouds over the tropical island of Puerto Rico have been studied over the course of many years, primarily with respect to the sources of cloud condensation nuclei (CCN). Puerto Rico has been the site of these studies because of the fair-weather, maritime flow and mostly clean atmosphere that leads to a mountaintop cloud that forms quite frequently throughout the year and can persist for several days (Allan et al., 2008; Gioda et al., 2013; Spiegel et al., 2014; Valle-Díaz, et al., 2016; Raga et al., 2016; Torres Delgado, 2021). In addition to the clean, maritime sources, the cloud studies have also identified particles produced from urban areas, locally on the island of Puerto Rico and upwind from islands to the east, where vehicular and industrial emissions produce anthropogenic particles with organic carbon and sulfate compounds (Allan et al., 2008). Apart from this, clouds and rainwater in this region are influenced by long-range transported natural aerosols, e.g., African dust, which is also potentially an important source of CCN, although the results are not conclusive as to how much cloud properties differ in the presence of these particles (Spiegel et al., 2014; Valle-Díaz, et al., 2016; Raga et al., 2016; Torres Delgado, 2021).

Airborne, primary biological aerosol particles (PBAP) are an important type of aerosol in the tropics (Gabey et al., 2010, 2013; Stanley et al., 2011) that can encompass viruses (0.01-0.3 µm), pollen (5-100 µm), bacteria and bacteria agglomerates (0.1-10 µm), and fungal spores (1-30 µm), as well as mechanically formed particles, such as dead tissue and plant debris (Finnelly et al., 2017). Furthermore, there is evidence that PBAP may influence the hydrological cycle and climate by initiating the ice nucleation process or acting as giant CCN (Möhler et al., 2007; Pope, 2010). Bioaerosols contribute a relatively small fraction (50 Tg yr^{-1}) of the total natural global emissions (~2900-13000 Tg yr^{-1}) (Hoose et al., 2010; Stocker et al., 2013); however, their mass and number concentrations are site specific and greatly vary depending upon the location and climatic conditions (Zhang et al., 2021 and references therein). In terrestrial ecosystems, bioaerosols constitute a major fraction, up to 30%, of total aerosol number concentration of coarse mode particles larger, i.e., those > 1 µm (Fröhlich-Nowoisky et al., 2016). There is additional evidence that this number fraction is even larger in the urban air (Jaenicke, 2005). Upon emission from the biosphere PBAP undergoes various physico-chemical changes (coagulation, photooxidation, surface coating, etc.) and are removed through dry and wet deposition. These large PBAP play a special role in precipitation development as giant CCN because they activate as larger droplets that more easily collide and coalesce to form raindrops. Hence, although small in number concentration, their size and capacity to contribute to early precipitation development make PBAP potentially significant aerosols that impact the hydrological cycle.

Puerto Rico is characterized by tropical climate, urban land cover and use, moist soils, unique topography, and dense vegetation. These factors, associated with the easterly trade winds from the East, influence the properties of atmospheric particles (Velázquez-Lozada et al. 2006). In addition, meteorology, i.e. humidity, temperature and winds, has an important role, especially during the rainy season when fungal spores are predominantly released. The air quality of Puerto Rico suffers at times as a result of anthropogenic activities, African dust storms and volcanic eruptions on nearby islands. Emissions from to the local pharmaceutical and power generation plants are responsible for releasing millions of pounds of air pollutant annually as well as a large number of organic compounds (e.g., n-alkanes, esters, phthalates, siloxanes, and other) including plasticizer released into the atmosphere, which could pose major health threat in this area (Torro-Heredia et al., 2020). The bioaerosol population on the island of Puerto Rico, and in particular in the capital city of San Juan, has been studied extensively using analysis of substrate samples (Quintero et al., 2010; Rivera-Mariani et al., 2011; Rivera-Mariani et al., 2020). The objective of the majority of these studies has been to evaluate the health effects of fungal and pollen spores on the local population (Quintero et al., 2010; Rivera-Mariani et al., 2011; Ortiz-Martínez et al., 2015; Rivera-Mariani et al., 2020). The studies by Quintero et al (2010) are particularly relevant to the investigation reported here because they classified a wide variety of fungal and pollen spores that were the most responsible for respiratory ailments suffered by the residents of San Juan. In addition, they could link the relative number concentration of these spores to meteorological factors like relative humidity and wind speed. Given that these prior studies demonstrated that bioaerosols are a significant contributor to the aerosol population in Puerto Rico, and that other studies have studied the role of marine aerosol and anthropogenic CCN in cloud formation over the island, the question arises if bioaerosol might also be an important source of CCN in this tropical region.

Prior to embarking on a longer-term project to evaluate PBAPs and CCN, under a wide range of conditions, a pilot study was designed and executed to investigate the properties of bioaerosols and CCN during September 2019. September was selected because not only did the Quintero et al. (2010) results show that this time of the year is when peak concentrations of bioaerosol spores are found, it is also a month of frequent cloud formation.

Considerable progress has been made in the development of technologies based on ultraviolet light-induced fluorescence (UV-LIF) (Ho, 1999; Huffman and Santarpia, 2017) for identifying PBAP that fluoresce when excited at UV wavelengths. The Wideband Integrated Bioaerosol Spectrometer (WIBS) and the Ultraviolet Aerodynamic Particle Sizer (UV-APS) are examples of such instruments that measure the optical properties of individual particles over a moderately large wide size range (Savage et al., 2017). The WIBS and the UV-APS have been used in studies such as the ice nucleation activity of bioaerosol (Twohy et al., 2016), measurement of fungal spore concentrations (Gosselin et al., 2016), and investigation of long-range transported bioaerosol in the tropics (Gabey et al., 2010; Whitehead et al., 2016) and high altitudes (Gabey et al., 2013). The WIBS was developed by the University of Hertfordshire and commercialized by Droplet Measurement Technologies, LLC. In parallel with the WIBS measurements, the CCN and condensation nuclei (CN) number concentrations were also measured to investigate the links between fluorescing aerosol particles (FAP), used here as proxies for bioaerosols, cloud forming particles and the total aerosol population, represented here by the CCN and CN measurements, respectively.

The primary objectives of this exploratory, pilot study are to 1) measure the number concentrations of CN, CCN and FAP, 2) identify correlations between CCN and FAP, 3) analyze trends related to meteorological factors, and 4) compare the FAP measurements with those from previous studies that documented fungal and pollen spores using off-line analyses.

2 Measurement and analysis methodology

2.1 Measurement site and experimental setup

The CN, CCN and FAP measurements were made (Fig. 1a) at the Facundo Bueso (FB) building on the University of Puerto Rico, Rio Piedras (UPR-RP) Campus (18°24'6.4"N, 66°03'6.5"W, 6 m a.m.s.l.). The spores were collected using the Hirst-type Burkard sampler (Burkard Scientific Ltd, Uxbridge, UK). located on the rooftop of the Medical Sciences Campus (MSC) of the University of Puerto Rico (18°23’48” N, 66°4’30” W, 60 m a.m.s.l). The university is located in the capital city of San Juan (pop. 2,448,000) which covers an area of 199 km^2. San

Juan has a tropical climate with an annual rainfall of 107±33 mm. The particles sampled at the measurement sites arrive from various sources, primarily from residential cooking, roadway traffic, and vegetation.

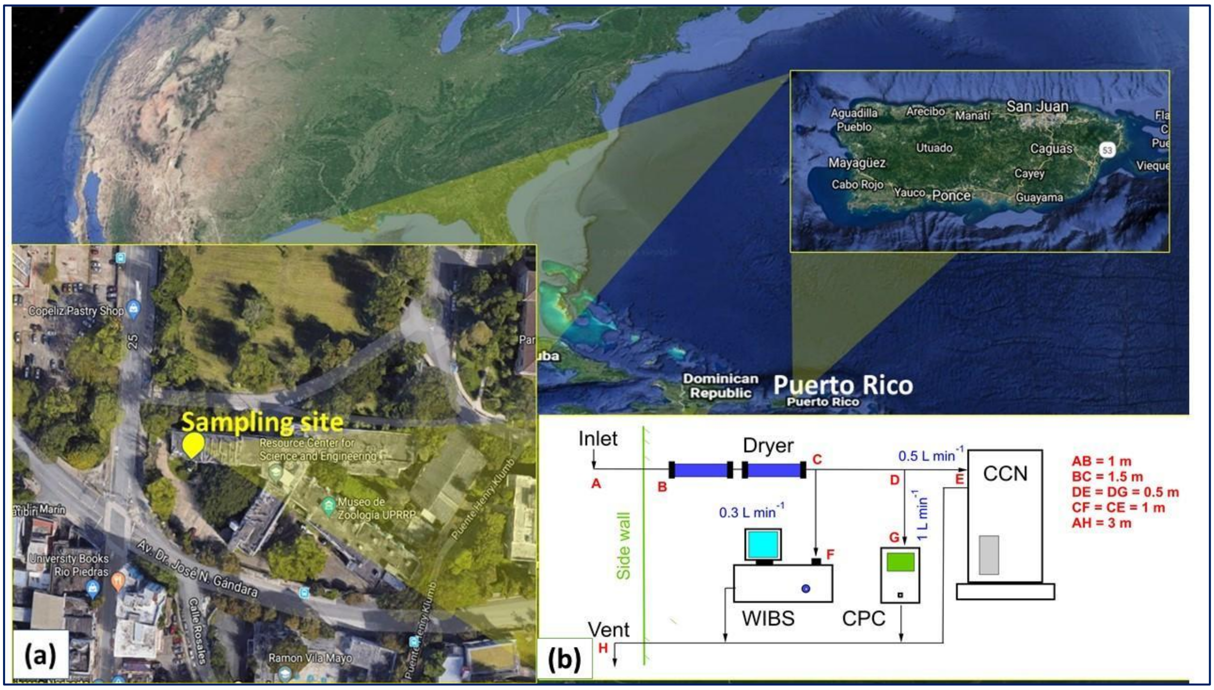

Figure 1. (a) Sampling location in the FB building of UPR-RP (b) experimental setup comprising the Cloud Condensation Nuclei counter (CCN), Condensation Particle Counter (CPC), and the Wideband Integrated Bioaerosol Spectrometer (WIBS). This figure was generated using © Google Earth Pro 7.3.

2.2 Instrumentation

Sampling was performed for eight consecutive days (September 16-23, 2019). The measurement setup consisted of two diffusion dryers (TSI model 3062) connected in series, a Cloud Condensation Nuclei Counter (CCN-100, Droplet Measurement Technologies), Condensation Particle Counter (CPC, TSI model 3772), and a Wideband Integrated Bioaerosol Spectrometer (WIBS-NEO, Droplet Measurement Technologies) (Fig. 1b). The samples were drawn from the exterior through the sidewall of the laboratory (~3 m above the ground) with conductive tubing (1/4” internal diameter and 1 m length). The aerosols were dried as they passed through two diffusion dryers (< 10% RH) containing silica gel before entering a manifold connected to the WIBS, CCN100, and CPC, which sampled at flow rates of 0.3, 0.5, and 1 L min^{-1}, respectively. Particle losses due to sedimentation, diffusion, and inertial separation along the sampling lines were calculated for each of the instruments (Kulkarni et al., 2011). The particle sampling efficiencies with respect to particle size are shown in the Supplement (Fig. S1). The sampling efficiency calculated for the particle size range 0.1-3 µm is greater than 80 %, decreasing to 60% at larger sizes. At this time there have been no corrections applied for these losses. The WIBS derives an equivalent optical diameter (EOD) from the light scattered by individual particles that pass through a focused laser beam. The EOD is defined as the size of a particle scattering the equivalent intensity of light as a spherical particle with known refractive index. Given that bioaerosols, dust and other types of environmental aerosols are not spherical, and their refractive index is unknown, the geometric size can be estimate to, at best, ±20%, hence relative size is more relevant than absolute size in our current analysis.

The CCN-100 is a continuous-flow, thermal-gradient, diffusion chamber that measures the concentration of aerosols activated as cloud droplets as a function of supersaturation (SS). Aerosol samples are drawn into a 50 cm tall column (inner diameter 2.3 cm) whose inner walls are saturated with water. A series of heaters along the column are controlled to maintain a gradient from colder to warmer temperatures as the particles move down the column. Since water vapor from the wetted column diffuses to the particles faster than the heat, a supersaturated condition is maintained that is determined by the temperature gradient and flow rate. Those aerosol particles that activate as cloud droplets at the constant SS in the chamber grow as the water molecules diffuse to the particle surfaces. An optical particle counter measures the number size distribution of the cloud droplets within the size range of 0.75–10 μm as the activated droplets exit the chamber. The detailed operating principles and calibration procedures are described by Roberts and Nenes (2005). In our study the supersaturation (SS) was maintained at 0.3%, a SS that is in the range of what would be encountered in convective clouds similar to those that form over the island of Puerto Rico (Duan et al., 2012: Uin et al., 2016).

The total concentration of environmental particles > 0.01 μm were measured with the CPC where the aerosol sample is drawn continuously through a heated saturator in which butanol vapor diffuses into the aerosol stream. An external vacuum pump was used to draw the aerosol samples at 1 L min^{-1}. This CPC employs a single particle count mode to measure the particle number concentrations up to 10^7 L^{-1} at an accuracy ±10%. The detailed design and working principle of the CPC are described by Stolzenburg and McMurry (1991).

The WIBS measures the fluorescent characteristics of aerosols using ultraviolet, light-induced fluorescence (UV-LIF) (Kaye et al., 2005; Stanley et al., 2011). This instrument provides detailed information on fluorescing bioaerosols on a single particle basis. The detection principles of the WIBS are discussed elsewhere (Kaye et al., 2005) and briefly described here. Atmospheric particles are drawn into the WIBS via a laminar flow delivery system and pass through the beam a continuous-wave diode laser (635 nm), which acts as a source for particle sizing and shape detection. The total flow is approximately 2.4 L min^{-1} of which 2.1 L min^{-1} is introduced in the form of sheath flow (i.e., filtered air) and 0.3 L min^{-1} is sample flow to maintain the particle alignment with the 635 nm laser. The forward scattering of the light is detected by a quadrant photomultiplier tube (PMT) and is used to determine the asphericity factor (AF) of the particles, which roughly estimates the shape of the particles (Gabey et al., 2010). Experimental evidence shows that the AF is near zero for a spherical particle, while it approaches 100 for a fiber or rod-like particle (Kaye et al., 2007; Gabey et al., 2010). The light scattered is used to activate, sequentially, two Xenon lamps that are filtered to illuminate the particles with 280 nm and 370 nm light, respectively. The wavelengths were specifically selected to excite fluorescence in particles containing tryptophan (280 nm) and nicotinamide adenine dinucleotide (NADH, 370 nm). Examples of molecules containing tryptophan or NADH are proteins, vitamins, large polymers, molecules having conjugated double bonds, heterocyclic aromatic compounds, particularly when nitrogenous substituents are present. Tryptophan is an amino acid that has the highest (~ 90%) fluorescence in the native protein. Nicotinamide Adenine Dinucleotide Phosphate (NAPDH) is one of the major contributors to the fluorescence signal when attached to the protein molecule and is produced widely in the metabolic cell. The fluorescence is recorded by the PMT detectors filtered at 310-400 nm and 420-650 nm. Hence, when a particle is excited at either of the incident wavelengths, there are four possible responses: 1) no fluorescence detected, 2) when excited at 280 nm the particle fluoresces at a wavelength in the 310-400 nm waveband (FL1), 3) when excited at 280 nm the particle fluoresces at a wavelength in the 420-650 nm waveband (FL2), or 4) when excited at 370 nm the particle fluoresces at a wavelength in the 420-650 nm waveband (FL3). The fluorescence characteristics of an individual particle are determined in any of the three fluorescence channels when its fluorescence emission intensity exceeds a baseline threshold. The baseline threshold is determined using the approach by Perring et al. (2015) that incorporates the daily data sets to remove background artifacts. Particles that exhibit fluorescence lower than the baseline threshold were treated as non-fluorescent particles. A particle that fluoresces when excited by either of the xenon lamps may also produce emissions in both the 310-400 and 420-650 wavelength; hence, from the FL1, FL2 and FL3 signals there are seven possible combinations that are designated fluorescence types A, B, C, AB, AC, BC, and ABC (Perring et al., 2015). Types A, B and C refer to particles that fluoresce only in FL1, FL2 and FL3. The other four types are the respective combinations of the A, B, and C.

It should be noted that the A and C types are highly sensitive to fluorescent bioaerosol particles whereas the B channel is cross sensitive to non-biological aerosols like certain organic compounds (Gabey, 2011). Based on the above description, the WIBS records the EOD, AF, fluorescent excitation-emission matrix and the total number concentration (N_{WIBS}), which includes non-fluorescing and total FAP within the size range from 0.5 to 30 µm. Before deployment the WIBS was factory calibrated for the size, sphericity and fluorescence using reference fluorescent polystyrene latex spheres which are traceable to National Institute of Standards and Technology (NIST).

Note, it is important to emphasize that although the WIBS was designed to detect fluorescence from biological particles, it is unable to unequivocally differentiate what type of bioaerosol fluoresced, e.g., if the particle was bacteria, fungus, or pollen. There are a number of studies, such as those by Hernandez et al. (2016), that have used the WIBS in laboratory studies to characterize a variety of species of bacteria, fungi, and pollen. Such studies have shown that these three types of bioaerosols fall in general categories of size and fluorescence type. These categories will be discussed further on in this paper in the context of comparing the FAP characteristics in San Juan to those reported in controlled laboratory experiments.

All measurements from the three instruments are averaged over five minutes intervals. In addition, the particle by particle (PbP) data from the WIBS are used to create size distributions and derive fluorescence properties and interrelationships in greater detail.

2.3. Fungal spore data

The fungal spore data were obtained from the department of Microbiology of the Medical Sciences Campus of the University of Puerto Rico. The enumeration of outdoor spores used the 12-traverse methodology proposed by the British Aerobiology Federation (Caulton and Lacey, 1995). Airborne spores were collected using a volumetric Hirst-type sampler, specifically a Burkard (Burkard Scientific Ltd, Uxbridge, UK). This equipment was located on the rooftop of the Medical Sciences Campus of the University of Puerto Rico, 30 meters above ground level. The Burkard 24-hr trapping system worked continuously with an intake of 10 L min^{-1}. Spores were impacted on a microscopic slide coated with a thin layer of 2% silicon grease as the trapping surface. The slides were changed daily and mounted on polyvinyl alcohol (PVA) mounting media for microscopic examination. Counting was done on each preparation along 12 traverse fields every 2 hours for a total of 12 hours on the longitudinal traverses. Spores were identified based on their morphological differences (Quintero et al. 2010). The identification was performed by means of a bright-field optical microscope NIKON Eclipse 80i microscope (Nikon Manufacturing), using a magnification of 1000X.

2.4. Meteorological data

Hourly meteorological data e.g., temperature (℃), relative humidity (RH, %), wind speed (WS, m/s) and wind direction (Degree) were provided by the department of natural science taken Twenty-four-hour air mass back trajectories, ending at 100 m above mean sea level, were obtained from the Hybrid Single Particle Lagrangian Integrated Trajectory Model (GDAS, 1-degree resolution, HYSPLIT) to identify the aerosol sources.

3 Results and Discussion

3.1 Time series

Figure 2a shows the temporal trends in particle number concentrations of CN, CCN (at 0.3% SS) and N_{WIBS} (0.5 - 30 µm) averaged in 10-minute intervals. The average particle number concentration measured by the CPC was $(3\pm1)\times10^6$ L^{-1}. This value is higher than the CN number concentrations reported previously at other more remote locations on the island, such as at the northeast coastal site of the Cabezas de San Juan nature reserve and at the Pico del Este, in El Yunque National Forest, where the CN concentrations were $(9\pm5)\times10^5$ and $(11.6\pm3)\times10^5$ L^{-1}, respectively, both as reported by Allan et al. (2008). The differences in CN concentrations are primarily related to the geographical locations. The university measurement site is an urban location influenced by anthropogenic emissions whereas the Cabezas de San Juan is a remote coastal location where the atmosphere is relatively clean, influenced by marine aerosols or long-range transported aerosols. The Pico del Este (East Peak) is a mountainous region that has a significant influence of aerosol from the nearby vegetation and from particles transported from marine boundary layer. The CN concentrations show systematic, daily trends that reflect the emissions from motorized vehicle traffic and nearby residential heating and cooking. The mean CCN concentration of $(1.5\pm0.5)\times10^5$ L^{-1} is about 20 times lower than the CN, suggesting that particles over the site are mostly non-hygroscopic or of low hygroscopicity, as would be expected of particles with anthropogenic origin, e.g., organic or black carbon.

The number concentrations of N_{WIBS} and FAP were $(7.3\pm5)\times10^4$ and $(5\pm3)\times10^3$ L^{-1}, respectively, which are approximately 40 and 600 times lower than the CN concentrations. Given the differences in the lower size thresholds for the CPC and WIBS with respect to the smallest detectable particle, 10 nm and 500 nm for the CPC and WIBS, respectively, this implies that about 98% of the particles are smaller than 500 nm. The FAP concentrations showed a systematic, daily cycle where nighttime particle concentrations were relatively higher than during the daytime. This trend is being driven primarily by the FAP type ABC, as illustrated in Fig. 2b where these concentrations are mostly much higher than the other six types. The type AB and AC concentrations have trends similar to the type ABC, although their absolute magnitudes are much lower.

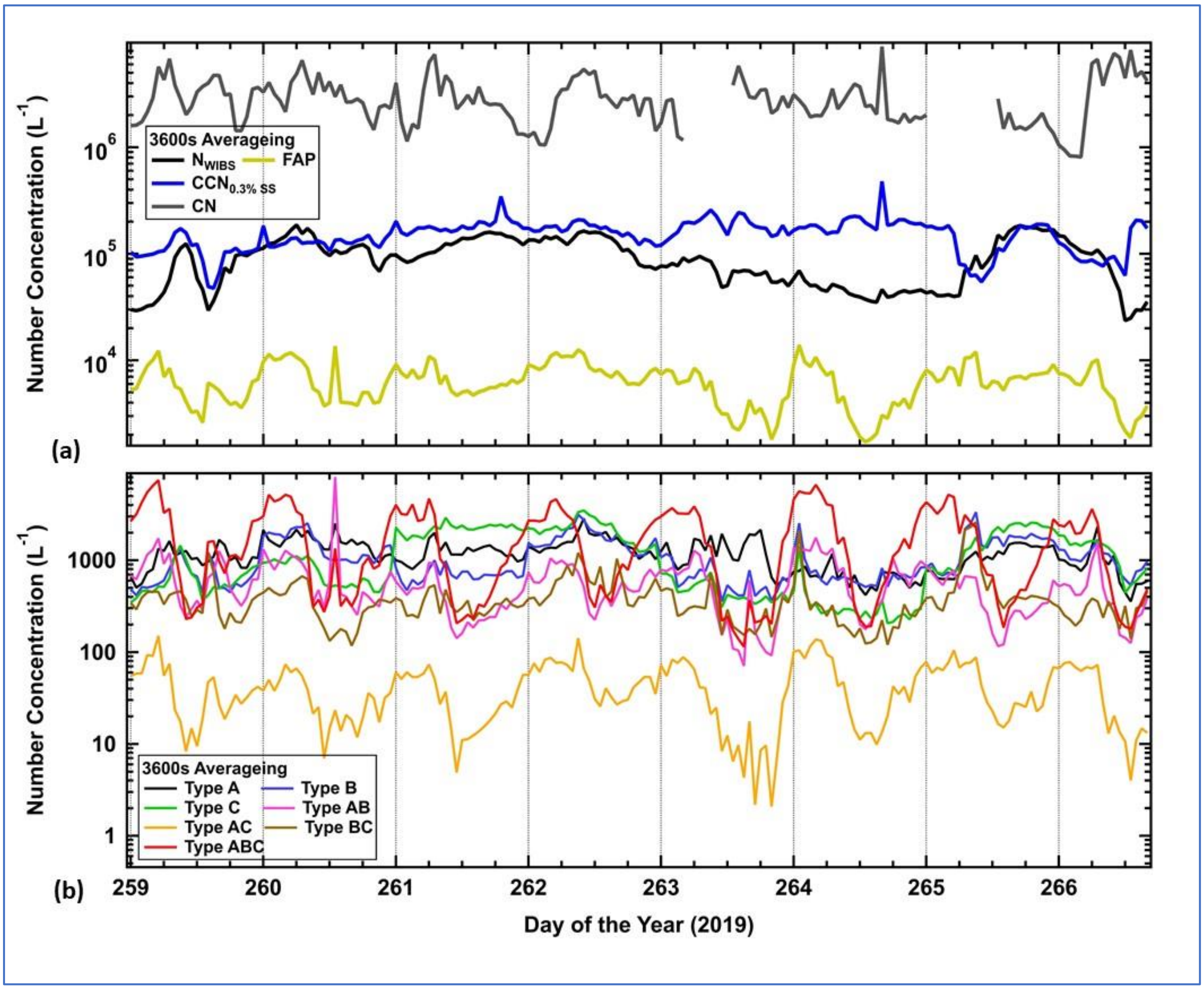

Figure 2. Time series of the number concentrations. (a) CN, CCN, N_{WIBS} and FAP. (b) FAP types A, B, C, AB, AC, BC, and ABC. The gaps in time of the CN concentrations were when the CPC was offline.

In the time series of number concentrations in Fig. 2 there are what appear to be periodicities in the CN, CCN and FAP. This periodicity is seen more clearly in the concentrations averaged by the time of the day (over the whole measurement period) as shown in Figs. 3a and 3b. Figure 3a highlights the diel trend in CN concentration (black curve) that reaches an initial peak at 7 am then a second peak four hours later at 11 am, local time. The CCN concentrations (blue curve) have morning peaks at 4 and 9 am followed by a peak of much higher magnitude at 4 pm. The N_{WIBS} (magenta) first peaks at 7 am, similar to the CN followed by a second maximum an hour after the CCN peak. The FAP concentrations remain elevated between midnight and 6 am, after which they decrease by about 30% and remain fairly constant the remainder of the day. The FAP are dominated by the Type ABC particles in the morning hours where their concentrations are four times larger than all other types, as shown in Fig. 3b.

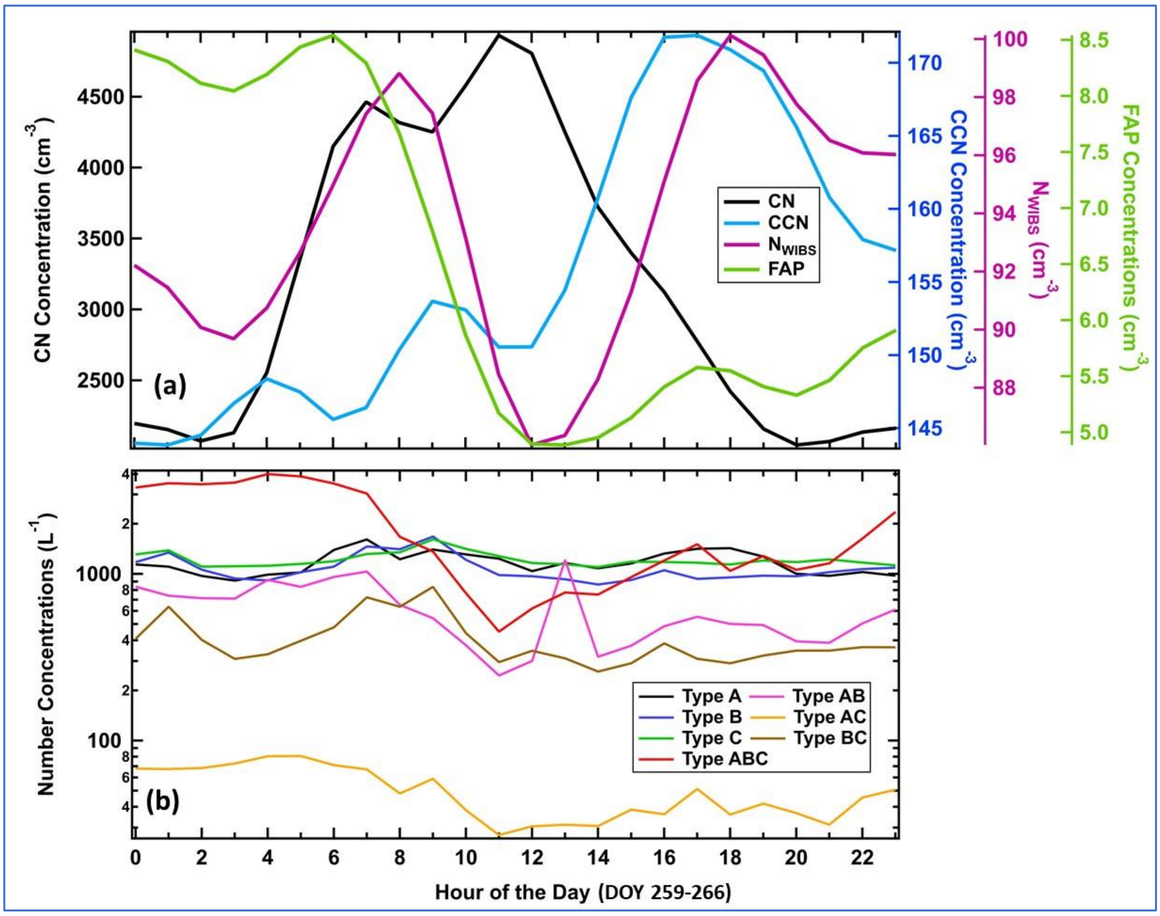

Figure 3. (a) Hourly concentrations of CN (black curve) and CCN at 0.3% supersaturation (solid blue curve), N_{WIBS} (magenta) and FAP (green) concentrations. (b) Hourly concentrations of the seven types of FAP.

All other FAP types remain approximately constant throughout the day except for the Type AC, which follows the trend of the Type ABC, but at significantly lower concentrations.

3.2 Temporal trends of the particle size distribution

Figure 4 shows the size distributions of total (Fig. 4a) and FAP (Fig. 4b) number concentrations averaged in 10-minute intervals. The color scale is the log of the concentration. The white curves are the average median volume diameters. The total number size distributions show an irregular trend of increasing concentrations over all sizes, usually occurring around midday on all days except on the day of the year (DOY) 264 when the size distributions remain approximately the same throughout the day. In contrast, the FAP size distributions have a more regular, daily pattern whereby the concentrations increase over all sizes to a maximum between midnight and 6 am. This reflects a similar trend that was illustrated in the daily FAP concentrations in Fig. 3a.

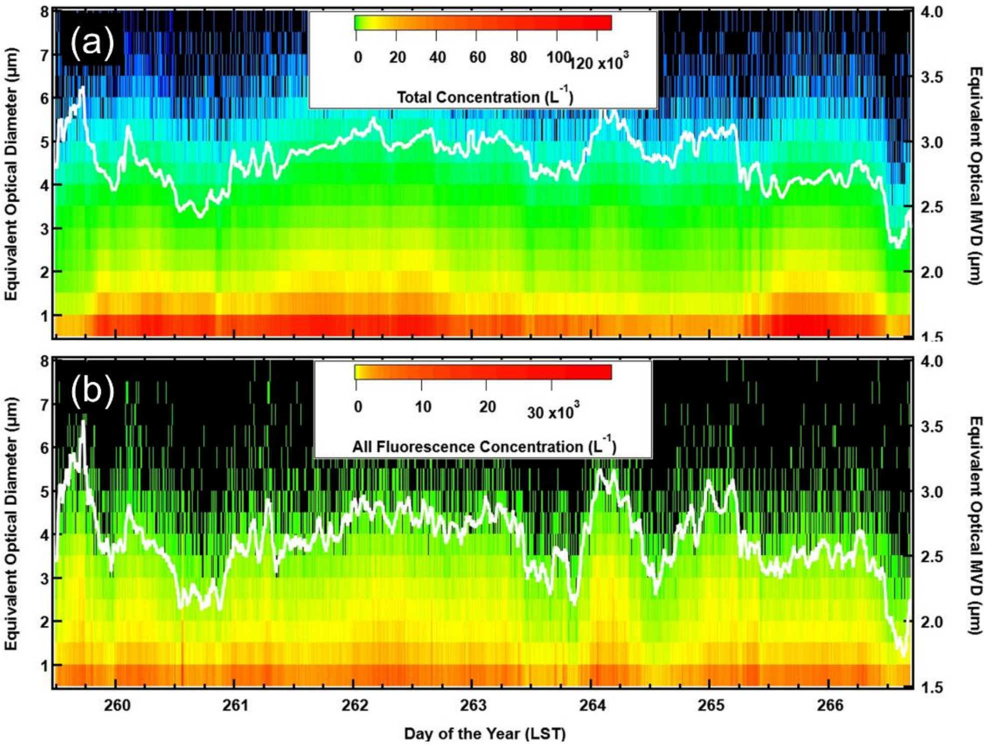

Figure 4. Time series of total (a) and (b) fluorescent particle size distributions measured by WIBS for the period September 16-23 (DOY 259-266), 2019. The white curves are the average median volume diameters (MVD).

The daily trends of the size distributions of the seven different types of fluorescent particles are shown in the Supplement (Fig. S2). where we observe that ABC and AB types were dominant at the site with a unique and systematic diel cycle. Reflecting the behavior of the total concentrations in Fig. 3b, the average EODs of ABC and AB type particles increase at night when the particle size grows to >4 µm by midnight. Fluorescent type A does not show any specific temporal trend while types B and C have periods when the concentrations increase over all sizes but do not follow the trends of the ABC and AB types particles. The type BC and AC particle concentrations are much lower than the other types.

The increases in the modal diameter from daytime to nighttime, seen in the Supplement (Fig. S2), particularly for the types AB, AC and ABC, was further investigated by comparing the size distributions averaged at night and in the daytime. We have plotted the particle size distributions for these three FAP types (Fig. 5), averaging from noon to 6 pm (red shading) and from midnight to 6 am (blue shading) over the whole measurement period (DOY 259-266). These two periods represent time intervals when the number concentrations and average sizes exhibit the largest differences. All three FAP types show a shift towards larger sizes from daytime to nighttime; however, the type ABC particles have the most distinctive shifts (Fig. 5c), indicative of both a general increase in concentration over all sizes but with a very clear, larger increase at EODs larger than 2 µm.

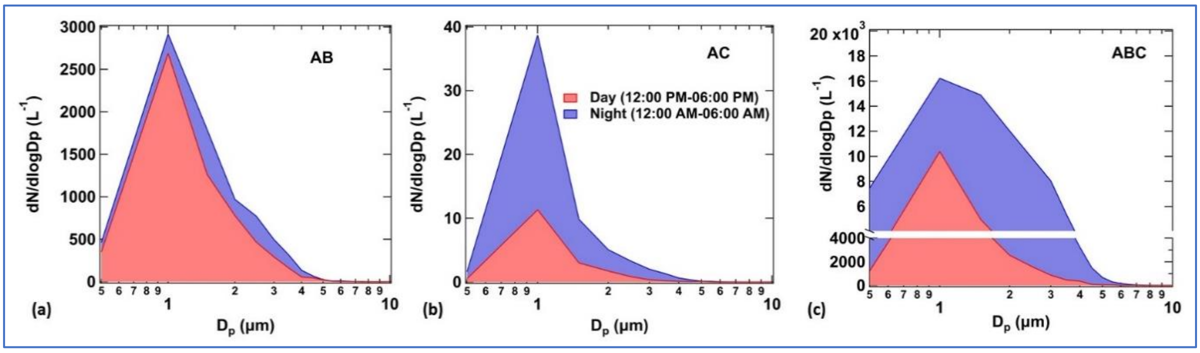

Figure 5. The size distributions of types (a) AB, (b) AC and (c) ABC were averaged from 12 pm to 6 pm (red shading) and from midnight to 6 am (blue shading) for the eight days of the project.

3.3 Asphericity

The asphericity, derived from the quad detector of the WIBS, is a relative indicator of the shape of each particle as shown in the supplement (Fig. S3) for FAP type (AB, AC, and ABC) and for all particles including the non-FAP. The color scale shows the average asphericity at each size interval over the duration of the project. Among the fluorescent types, the asphericity of

ABC particles shows the most dominant mode between 2 and 4 µm during nighttime, especially at midnight. The asphericity size distributions of all particles show a broader mode of enhanced asphericity between 2 and 4 µm that varies somewhat but not in a noticeable diel pattern. Note that particles with asphericities < 20 are generally considered quasi-spherical so that the values that are shown here indicate slight changes in shape, on average, of type ABC particles, as well as all particles, but the overall population of particles can be considered quasi-spherical.

The asphericity of non-fluorescent (non-FAP) particles was always observed higher than the FAP (Fig. S3d in the Supplement). The higher asphericity values of non-FAP particles can be seen between size 3 and 6 µm every day and dominate on DOY 261 and 262.

3.4 Air mass back trajectories

The air masses that arrived at the measurement site on DOY 259 and 264 had been over the Atlantic Ocean, northeast of the island, 24 hours earlier while on DOY 260-63 and 266 they were arriving from the southeast and on DOY 265 they were from the south-southeast. Figure S4a shows that the air masses on all days had been < 50 m above the surface the entire 24-hour period before arriving at the measurement site. The one exception was on DOY 259 when the air mass had stayed above 200 m from 12 to 24 hours then began descending as it approached the island. This same air mass was associated with rain formation close to the measurement site (Fig. S4b in the Supplement). The air mass on DOY 264 came across the islands to the SE of Puerto Rico (e.g., Culebra and the British Virgin Islands), possibly mixing the marine aerosols with polluted emissions before arriving at the measurement site. Likewise, the air mass trajectory on DOY 260 and 262 crossed over the Vieques and US Virgin Islands at a low altitude, also mixing with anthropogenic emissions. The increment in total particle number concentrations on DOY 260-262 and DOY 266, shown in Fig 4a, is possibly attributed to these air mass that passed over the populated islands to the southeast of Puerto Rico and may also be the reason why we observed higher values of asphericity of non-FAP on DOY 261 and 262. The remainder of the air masses were presumably not impacted by anthropogenic emissions until arriving over the Puerto Rico landmass.

3.5 Meteorological data

Figure S5 shows the temperature and relative humidity (RH) (Fig. S5a), and the wind speed, wind direction and precipitation (Fig. S5b). The average wind speed, temperature, and RH for the period of measurement were 2.8±2.4 m/s, 29±2 ℃, and 77±11 %, respectively. The DOY

259 and 265 received significant rainfall of 34 mm and 47 mm, respectively. Note that these two days are associated with those air masses whose analysis indicated precipitation along their back trajectories. The wind speed and direction, temperature, and RH show a systematic daily cycle where the wind speed and temperature peaked during midday (2.8±0.7 m/s and 33±1℃), and the RH peaked around midnight (91±3 %). At the measurement site the winds were from 135°- 250° during the night shifting to 93°-134° during the daytime. On DOY 262 and 265, as well as the afternoon of DOY 259, the winds were comparatively low at night (0.24±0.2 m/s) compared to those during the day (2.8±0.6 m/s) suggesting generally calm wind conditions that are normal this time of year when not under the influence of tropical storms.

To further highlight the relationships between the meteorological conditions and FAP we computed the hourly averages of RH, wind speed and FAP concentrations during each 24-hour period over the eight-day period (Fig. 6a). The RH and FAP concentrations reach their maxima between the hours of midnight and 6 am while the wind speed is at a minimum during those hours.

The relationship between RH and the FAP fraction is highlighted in Figs. 6b and c where there appears to be an RH threshold of approximately 80% below which the FAP fraction remains lower than 0.1. When the RH exceeds this value the FAP fraction increases rapidly to its maximum value of 0.3. The color coding indicates the median volume diameter (Fig. 6b) and number concentration (Fig. 6c). In both cases the size and concentrations increase when the RH exceeds 80% The increase of FAP D_{mvd} and the number concentrations depend on the hygroscopicity of the particles. Among the different FAPs measured at the site, the ABC, AB, and AC types were observed to have systematic diel patterns and were believed to be more hygroscopic than others. Therefore, the D_{mvd} and FAP number concentrations were increasing when RH reaches 80% and above.

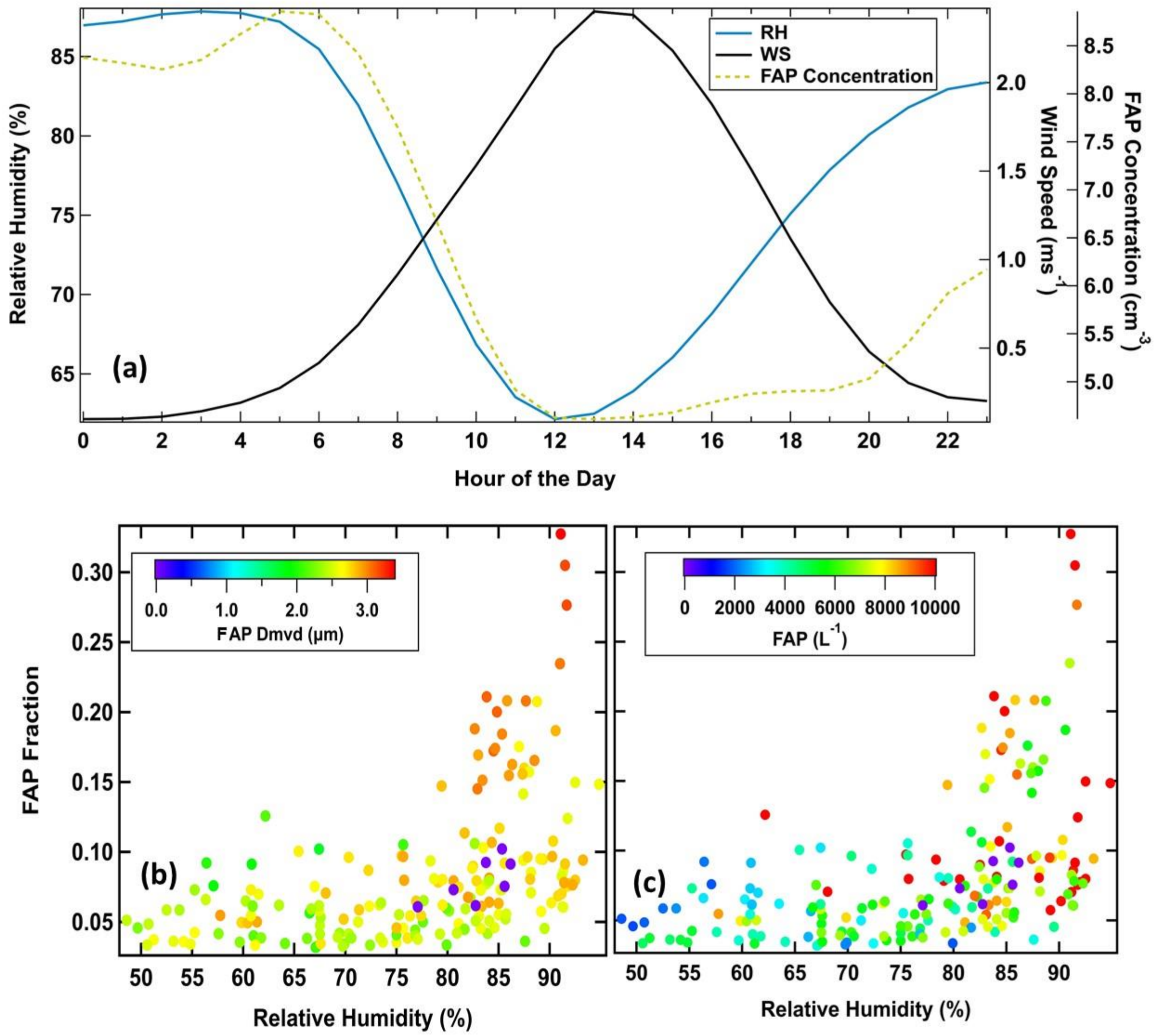

Figure 6. (a) hourly averages of relative humidity (blue curve), wind speed (black) and FAP concentration (green dotted). (b) link between fluorescent fraction and relative humidity (FAP particle volume weighted equivalent optical diameter. D_{mvd}, on the color scale). (c) fluorescent fraction and relative humidity (FAP particle concentration on the color scale). The data in all the figures averaged over DOY 259-266.

3.6. Fungal spore data

The time series of the Hirst sampler fungal spores are shown in Fig. 7. Similar to the FAP number concentrations and fractions, the spore concentrations have a diel trend with average concentrations of 48±42 L^{-1} and a maximum of 112±44 L^{-1} around midnight. We calculated positive correlations of 0.7, 0.47, and 0.54 between the total spore concentration and concentrations of FAP types ABC, AB, and AC, respectively. Previous studies for this region reported the most common fungal genera detected were the Basidiospores and Ascospores

(Quintero et al., 2010; Rivera-Mariani et al., 2011). Figure 7b illustrates how these fungal spore types were speciated. The broad categories are hyphae or filamentous spores, macroconidia >10 µm, microconidia 3-10 µm, microconidia < 3 µm, and unidentified spores. We observed that the microconidia 3-10 µm contributed the highest (81%) fraction to the total fungal species followed by microconidia (<3 µm) 3.86% and Macroconidia (>10 µm) 1.8%. The Basidiospores contributed the highest (49.4%) fraction to the total fungal spores, followed by Ascospores 19%, Diatrypaceae 8.6% and Penicillum/Aspergillus 3.86%. The mean concentrations of dominant species such as Basidiospores, Ascospores, Diatrypaceae and, Penicillum/Aspergillus were 24±20, 9.3±4, 4±3 and 2±1 L^{-1}. The Ascospores and Penicillum/Aspergillus had more elevated concentrations during the night while Diatrypaceae concentrations were generally higher during the daylight hours.

These species were the most common airborne spores in San Juan throughout the year and predominated during September (the rainy month); hence the FAP types ABC and AB, measured by the WIBS, were likely the Basidiospores and Ascospores (Fig. 7b). Previous studies (Quintero et al., 2010; Rivera-Mariani et al., 2020) reported that the most common fungal genera detected were the Basidiospores and Ascospores, confirmed in this study. The sizes of the Basidiospores and Ascospores (10-20 um) are usually larger than those of Aspergillus, Penicillium, and Cladosporium spores. Furthermore, we observed a systematic diel pattern in the number concentrations of these fungal spores, which is strongly correlated to diel pattern of FAP Type ABC. The other genera most frequently detected were the Penicillium/Aspergillus, Cladosporium and Ganoderma, observed at low concentrations reported by Quintero et al. (2010). Those species possibly corresponded to FAP type AC which were periodic but at relatively low concentrations. These fungal spores that occurred between the midnight and early morning period, suggest an active release mechanism induced by the high humidity during early morning hours under calm wind conditions, in concordance with the findings reported by Quintero et al. (2010).

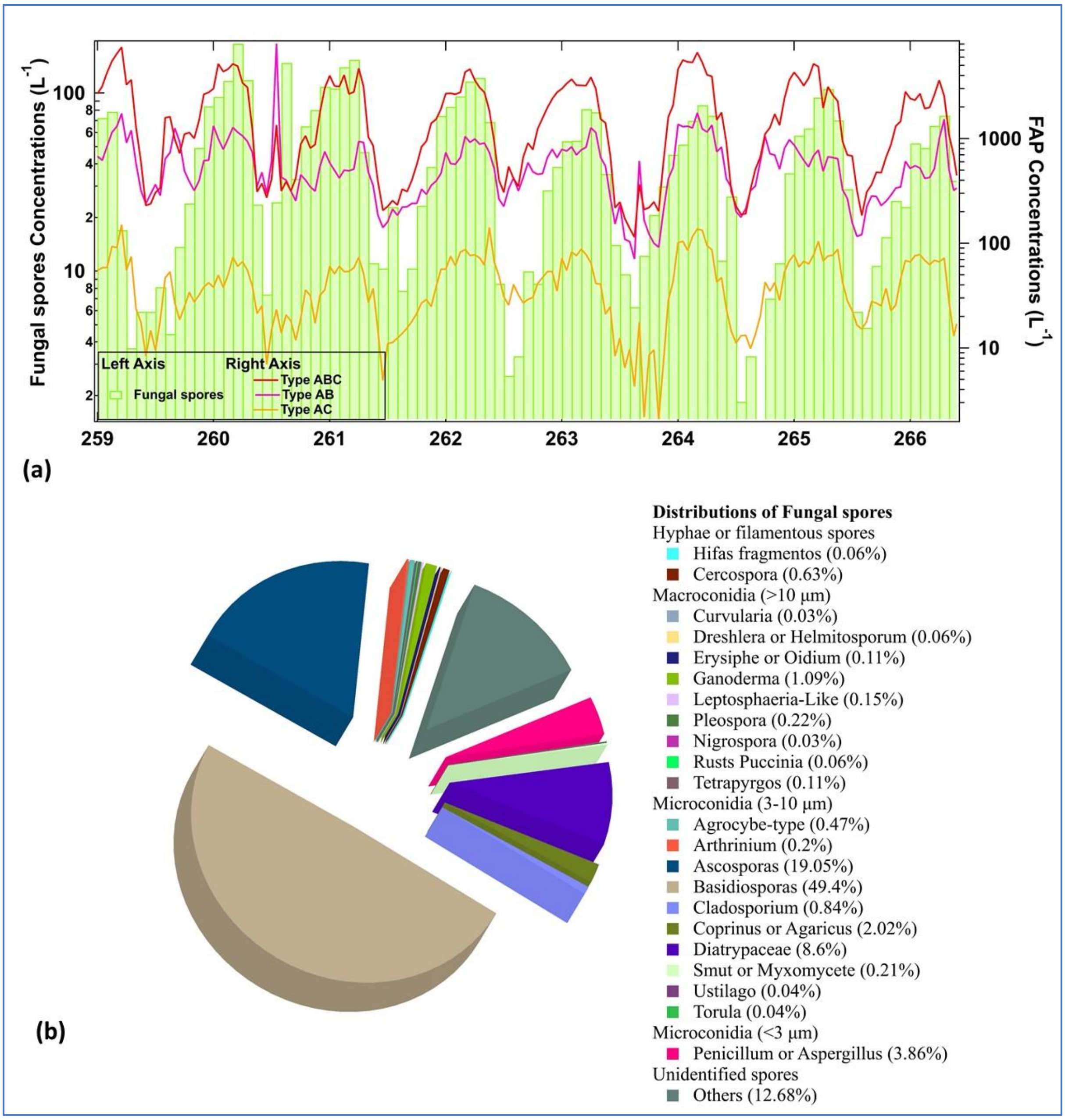

Figure 7. (a) time series of the particle number concentrations of fungal spores (left axis) measured at the Medical science department and the FAP types ABC, AB and AC (right axis) detected by WIBS. (b) Speciation of outdoor the fungal spores.

4. Discussion

The preliminary results from this pilot study highlight the following: 1) The CN, CCN and FAP concentrations have daily patterns during which each maximizes at a different hour of the day, 2) the periodic FAP concentration is predominantly of the type ABC that reaches a daily maximum around midnight during which the asphericity of this type also increases, 3) the RH reaches a maximum each day also around midnight, 4) the wind speeds are a minimum around midnight and 5) an independent analysis of bioaerosols using fluorescence microscopy to identify spore types revealed a periodicity of spore concentrations that was highly correlated with the RH and FAP type ABC concentrations.

Referring back to Fig. 3a, the CN, CCN, $N_{WIBS,}$ and FAP concentrations all exhibit a diel periodicity but with differing, uncorrelated trends. The CN population encompasses all environmental particles larger than about 10 nm and are dominated by anthropogenic aerosols. Given that the WIBS measures the concentration of particles larger than 0.5 µm, and that the total concentration has an average peak maximum of 100 cm^{-3}, compared to a maximum CN concentration 5000 cm^{-3}, this implies that 98% of the particles have sizes smaller than 0.5 µm. A comparison of the maximum CCN and N_{WIBS} concentrations, 170 cm^{-3} vs 100 cm^{-3}, leads us to conclude that most of the CCN are likely in sizes greater than 0.5 µm. Likewise, since the maximum CCN concentrations are only about 2% of the CN values, this suggests that most of the CN have low hygroscopicity, a characteristic of fresh combustion particles.

The timing of the maxima in the CN concentrations suggest that the trends are a result of two traffic patterns: the general city traffic as workers commute to jobs that are not on the university campus and vehicular traffic of university workers whose starting hours are later than the city workers. As shown in Fig. 1a, the sampling site is located near the intersection of two major avenue that carry both types of traffic.

The comparison between the times of the two N_{WIBS} maxima and the CN and CCN peaks suggests that the > 0.5 µm particles measured with the WIBS in the morning are a different mixture of compositions than the particles in the afternoon. The morning N_{WIBS} peak lags the first CN peak by an hour, likely as result of the primary emissions producing particles that grow into the size range of the WIBS; however, with the sunrise at around 6 am, temperatures begin increasing and the material in the more volatile particles begin to evaporate until the particle sizes decrease below the threshold of the WIBS. Some dilution will be occurring as the boundary layer deepens with increasing temperatures, but this is a secondary effect as we do not see the CN concentrations decrease with the decrease in N_{WIBS}. Since the CCN concentrations remain low during this period, this implies that either the particles did not grow large enough to be good CCN or their composition is non-conducive for forming CCN. In the early afternoon we observe the CCN concentrations increasing until reaching their late afternoon peak. The N_{WIBS} follows a similar trend but lags with respect to the CCN by a couple of hours. This afternoon trend in CCN has been identified in other large, polluted urban areas as the result of photochemical reactions producing hygroscopic, secondary organic aerosols (SOA) from photochemical reactions (Baumgardner et al., 2004). The N_{WIBS} is offset a couple of hours due to the time needed for the SOA particles to grow by condensation and aggregation. Finally, the FAP concentrations only begin increasing late in the evening after the CCN has maximized and the FAP concentrations are less than 10% of the CCN. This suggests that if FAP are good CCN, they do not contribute significantly to the overall CCN population. It is important to note that contributions to the overall CCN populations depend on size, chemical composition, and number concentrations of particles.

Quintero et al. (2010) concluded that the release of the fungal spores, those that they measured and speciated in multiple locations, was triggered by high RH. Pollen spores, on the other hand, could not be linked conclusively to any meteorological factor. Based on a comparison of the species of spores found at the university, compared with those measured in the El Yunque rain forest, Lewis et al (2019) concluded that the rain forest was the likely source of the majority of spores identified in the city of San Juan, and hence at the university. Two of the air sampling sites, Pico Del Este (PDE) and Cabezas de San Juan (CSJ) are very similar and very low in the fungal spores (less than 5,000 spores/m^3). At another sampling site in El Verde (located to the west within El Yunque National Forest), the concentrations increase to 72,000 spores/m^3 and are found to have a decreasing gradient of fungal spores towards the Metro Area. For the rest of Puerto Rico, the Central Mountain Range is the other major source of fungal spores. Hence, given these previous results, in comparison with the correlations that we have observed in the current study (Figs. 6 and 7), the type ABC fluorescing particles are most clearly linked to Basidiospores and Ascospores, the two species that made up the largest fraction of fungi measured with the fluorescence microscopy. The hourly averages in Fig. 3b also showed that the type ABC only was predominant during the same period as the Basidiospores and Ascospores while the other FAP types showed no obvious daily trends. This is mirrored by the spore types shown in Fig. 7 that change in relative mixture during the day.

The WIBS characterizes the fluorescent aerosol particles using two-wavelength excitations and two-wavelength emissions. The sensitivity of types A and B to the intensity of the emissions in the 310-400 and 420-650 nm wavelength bands, when excited at 280 nm, in comparison to the intensity of emissions at 420-650 nm when excited at 370 nm has been exploited in the study by Ziemba et al. (2016) to identify differences in bioaerosol types as they relate to differences in FAP sources. In their study they were able to show a clear grouping of FAPs linked to source regions by plotting the ratio of type A to type B (emission sensitive) versus the ratios of type C to type B (excitation sensitive). We have followed a similar scheme; however, whereas the Ziemba et al (2016) study used a WIBS on an airborne platform flying over various land usage types, our site was fixed so we compute these ratios as a function of time rather than location. Figure 8 illustrates the periodicity of the type C to B ratio, increasing during those time periods that the type ABC concentrations were also increasing. Just as the sizes of FAP were seen to increase during these periods (Fig. 5), indicative of a change in FAP type, the shift in the type C/type B reflects the differences in the fungal spore types.

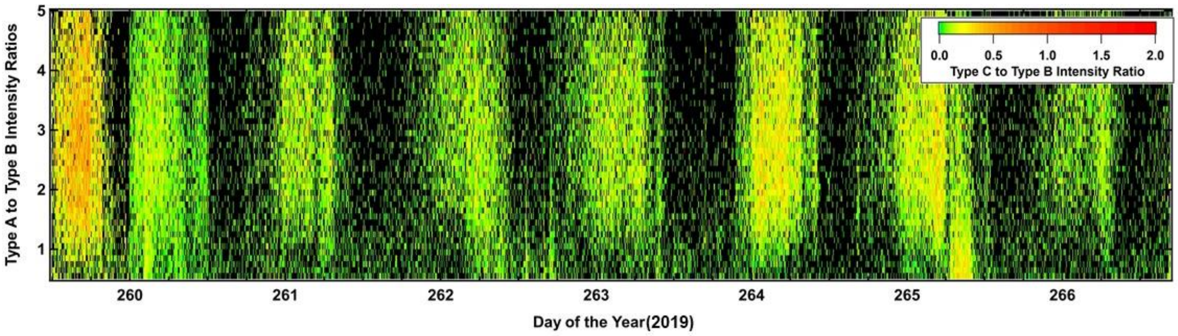

Figure 8: Temporal distribution of emissions wavelength dependence (Type A to Type B) vs excitation wavelength dependence (Type C to Type B).

Hence, the changes in size distribution, asphericity, type C/B ratios, and speciated spore concentrations, all occurring during the same time of day, provide independent verification that a different type of PBAP is being produced during the periods of high RH than during the other periods of the day.

The strong correlation between spore release and RH that has been highlighted in this study has been previously reported, e.g., (Oliveira et al., 2005; Chi and Li, 2007; Gabey et al., 2013; Calvo et al., 2018, Toprak and Schnaiter, 2013; Healy et al., 2014). None of those studies, however, were from tropical regions nor did they include the asphericity and FAP type ratioing to quantify their results.

Some laboratory studies have been conducted to measure the fluorescence characteristics of a small variety of bacteria, fungi, and pollen, for example Hernandez et al. (2016) determined that bacteria, fungi and pollen could be generally grouped according to the size and FAP type. In their study, very few fungal spores were of the FAP type ABC such as found in the current study. Instead, the majority of their fungi were types A and AB while the majority of type ABC spores were pollen, not fungi. On the other hand, the Hernandez et al. (2016) study did not test any of the major fungi species that were measured in the natural environment of Puerto Rico, i.e. Basidiospores and Ascospores. Hence, new laboratory studies with the WIBS measuring fungal spores native to Puerto Rico should be a high priority for future research.

5. Summary and Conclusions

A pilot study was conducted to evaluate the fluorescence and cloud condensation nuclei (CCN) properties of urban aerosols in San Juan, Puerto Rico, the first time such measurements have been made in this tropical city. Previous CCN measurements have been made on this island at coastal and rainforest sites, but no research has been pursued to see if bioaerosols are directly linked to CCN. There have been a number of laboratory studies conducted by other researchers who evaluated the CCN activity of various bacteria, fungi and pollen. Although some types of bioaerosols were found to be potential CCN, many others were not. Hence, the importance of bioaerosols as cloud forming particles remains an open question. The very large concentrations of fungal spores produced by flora in Puerto Rico, as reported by Quintero et al. (2010), along with the results from our pilot study, provided the initial motivation for the study reported here to assess if bioaerosols might contribute to the frequent cloud formation over the island.

The measurements were made from the Facundo Bueso building within the University of Puerto Rico, Rio Piedras Campus, from September 16-23, 2019, an urban location that experiences emissions from anthropogenic activities and the production of fungal spores from a wide variety of flora within the university campus as well as from the nearby tropical forest.

In the pilot experiment, the CCN and FAP concentrations were measured with a commercial CCN spectrometer and Wideband Integrated Bioaerosol Spectrometer (WIBS), respectively. It is important to note that bioaerosols are not the only type of aerosol particles that will autofluoresce when excited at the wavelengths used in the WIBS, although care was taken to minimize interference from non-biological particles. Therefore, what is reported in the current study are the properties of fluorescing aerosol particles (FAP) without specifically labeling them as biological. In addition to measurements of CCN and FAP, the total concentration of condensation nuclei (CN) was documented with a condensation particle counter.

The mean number concentration measured by the CCN counter at 0.3% SS was $(1.5 \pm 0.5) \times 10^5$ L^{-1}, which was about a factor 20 lower than the average CN concentration $(3 \pm 1) \times 10^6$ L^-

^{1}. The mean FAP concentration was $(5 \pm 3) \times 10^3$ L^{-1}, which was a small fraction (~7%) of the total aerosol particle number concentration, N_{WIBS}, measured by the WIBS, whose lower size threshold is 0.5 µm.

The CN, CCN, N_{WIBS}, and FAP concentrations all have daily trends but their maxima occur at different times of the day. The CN peaks at 6 am and 11 am due to business traffic and university traffic that have different rush hours. The CCN reaches its maximum value at 4 pm as photochemical processes produce secondary organic aerosols (SOA) that are likely hygroscopic in composition. The N_{WIBS} is bimodal with the morning peak at 8 am, reflecting rush hour emissions whose particles grow into the size range of the WIBS and then the second maximum at 6 pm as the SOA grow to measurable sizes. The diel trends in the FAP concentrations are not correlated with the CN, CCN or N_{WIBS} as they remain fairly constant throughout the daylight hours but then rapidly increase to their maximum value that extends from midnight until 6 am.

The FAP are classified according to the wavelengths at which they were excited and at which they emitted fluorescence. These types have been categorized as A, B, C, AB, AC, BC, and ABC. In the current study the types A, B, C and ABC all had average concentrations during the daylight hours of about 1000 L^{-1} while the other three types were much lower in concentration; however, only the type ABC showed the rapid increase in concentration, to almost 5000 L^{-1}, between midnight and 6 am.

Independent measurements using fluorescent microscopy of spores captured on substrates were made during the same time period. Although more than 20 species of spores were identified with this technique, the fungi Basidiospores and Ascospores were not only the most predominant, but they were also the spores that followed an almost identical daily trend as the FAP type ABC, i.e., remaining nearly constant in concentration during the daylight hours then increasing in the evening to their maximum between midnight and 6 am.

The other environmental parameters that also correlated significantly with the temporal trends in fungal spores and FAP were the relative humidity (RH) and the wind speed. As the RH began to increase in the late afternoon, the spore counts and FAP concentrations increased, as well. A comparison of RH with FAP concentrations indicates that the FAP concentrations begin increasing above an RH threshold of about 80%. Spores are released by a number of species of fungi when the RH increases, as has been well documented in other studies (Quintero et al., 2010). Hence, the relationship between RH, Basidiospores and Ascospores and the type ABC FAP has been clearly established.

Three additional properties of the FAP were extracted from the WIBS measurements that provided indirect but complementary information showing how the type ABC particles were related to the Basidiospores and Ascospores: 1) the size distribution, 2) the asphericity and 3) the excitation and emission sensitivity parameters. The type ABC particles during the high RH periods had much higher concentrations of particles larger than 2 µm when compared to the size distributions of these same particles in the daylight hours. Secondly, the asphericity increased during the high concentration of type ABC periods. Thirdly, the excitation/emission sensitivity parameters increased during this same period. While not quantitative, these three parameters confirmed that the particles whose concentrations were increasing had different properties than during other periods of the day.

Since the trends in the CCN concentration were not directly correlated with the FAPwe cannot conclude that bioaerosols are a potential source of cloud forming particles. In addition, the FAP concentrations were less than 10% of CCN concentrations, so that even if some FAP are potential CCN, the clouds that develop over the island are more likely formed from other aerosol types than locally produced fungal spores.

The results from this pilot study have provided strong motivation for longer term measurements that will expand the database of aerosol particle properties in this tropical, urban area. The detailed information on fungal spores in this region, in comparison with the multi-parameter data available from the WIBS, will improve our ability to interpret these measurements of FAP and apply this knowledge to data sets acquired in other parts of the world.

Data availability

Data used to support the findings in this study have been uploaded and are publicly available via Mendeley at https://data.mendeley.com/datasets/t26dctfk7t/1 (Sarangi et al., 2021).

Author Contribution

BS designed the study in consultation with OLMB and performed the measurements. BBR provided the measurements of fungal spores and pollen concentrations. DB and BS performed the analysis, interpreted the results and wrote the paper with contributions from OLMB and BBR.

Acknowledgements

This research was supported by NSF MRI grant (1829297) and NSF EAR Grant (1331841). The authors acknowledge the Droplet Measurement Technologies, Inc., Boulder, Colorado for providing training on instruments that are part of the NSF MRI project. The authors gratefully acknowledge the NOAA Air Resources Laboratory (ARL) for the provision of the HYSPLIT transport model (http://www.ready.noaa.gov).

Reference

Allan, J. D., Baumgardner, D., Raga, G. B., Mayol-Bracero, O. L., Morales-García, F., García-García, F., Montero-Martínez, G., Borrmann, S., Schneider, J., Mertes, S., Walter, S., Gysel, M., Dusek, U., Frank, G. P. and Krämer, M.: Clouds and aerosols in Puerto Rico - A new evaluation, Atmos. Chem. Phys., 8, 1293–1309, doi:10.5194/acp-8-1293-2008, 2008.

Baumgardner, D., Raga, G. B. and Muhlia, A.: Evidence for the formation of CCN by photochemical processes in Mexico City, Atmos. Environ., 38(3), 357–367, doi:10.1016/j.atmosenv.2003.10.008, 2004.

Calvo, A. I., Baumgardner, D., Castro, A., Fernández-González, D., Vega-Maray, A. M., Valencia-Barrera, R. M., Oduber, F., Blanco-Alegre, C. and Fraile, R.: Daily behavior of urban Fluorescing Aerosol Particles in northwest Spain, Atmos. Environ., 184, 267-277, doi:10.1016/j.atmosenv.2018.04.027, 2018.

Caulton E and Lacey M.: Airborne Pollens and Spores. A Guide to Trapping and Counting, 1st ed., British Aerobiology Federation (BAF) Publishers, 1995.

Chi, M. C. and Li, C. S.: Fluorochrome in monitoring atmospheric bioaerosols and correlations with meteorological factors and air pollutants, Aerosol Sci. Technol., 41, 672-678, doi:10.1080/02786820701383181, 2007.

Cziczo, D. J., Thomson, D. S., Thompson, T. L., DeMott, P. J. and Murphy, D. M.: Particle analysis by laser mass spectrometry (PALMS) studies of ice nuclei and other low number density particles, Int. J. Mass Spectrom., 258, 21-29, doi:10.1016/j.ijms.2006.05.013, 2006.

Drewnick, F., Dall'Osto, M. and Harrison, R.: Characterization of aerosol particles from grass mowing by joint deployment of ToF-AMS and ATOFMS instruments, Atmos. Environ., 42(13), 3006–3017, doi:10.1016/j.atmosenv.2007.12.047, 2008.

Duan, J., Chen, Y. and Guo, X.: Characteristics of aerosol activation efficiency and aerosol and CCN vertical distributions in North China, Acta Meteorol. Sin., 26, 579–596, doi:10.1007/s13351-012-0504-6, 2012.

Fennelly, M. J., Sewell, G., Prentice, M. B., O'Connor, D. J., and Sodeau, J. R.: The Use of Real-Time Fluorescence Instrumentation to Monitor Ambient Primary Biological Aerosol Particles (PBAP), Atmosphere, 9, 1–39, https://doi.org/10.3390/atmos9010001, 2017.

Fröhlich-Nowoisky, J., Kampf, C. J., Weber, B., Huffman, J. A., Pöhlker, C., Andreae, M. O., Lang-Yona, N., Burrows, S. M., Gunthe, S. S., Elbert, W., Su, H., Hoor, P., Thines, E., Hoffmann, T., Després, V. R. and Pöschl, U.: Bioaerosols in the Earth system: Climate, health, and ecosystem interactions, Atmos. Res., 182, 346-376, doi:10.1016/j.atmosres.2016.07.018, 2016.

Gabey, A. M.: Laboratory and field characterization of fluorescent and primary biological aerosol particles, Ph.D. thesis, University of Manchester, England, 2011.

Gabey, A. M., Gallagher, M. W., Whitehead, J., Dorsey, J. R., Kaye, P. H., and Stanley, W. R.: Measurements and comparison of primary biological aerosol above and below a tropical forest canopy using a dual channel fluorescence spectrometer, Atmos. Chem. Phys., 10, 4453–4466, doi:10.5194/acp-10-4453-2010, 2010.

Gabey, A. M., Vaitilingom, M., Freney, E., Boulon, J., Sellegri, K., Gallagher, M. W., Crawford, I. P., Robinson, N. H., Stanley, W. R., and Kaye, P. H.: Observations of fluorescent and biological aerosol at a high-altitude site in central France, Atmos. Chem. Phys., 13, 7415–7428, https://doi.org/10.5194/acp-13-7415-2013, 2013.

Gioda, A., Mayol-Bracero, O. L., Scatena, F. N., Weathers, K. C., Mateus, V. L. and McDowell, W. H.: Chemical constituents in clouds and rainwater in the Puerto Rican rainforest: Potential sources and seasonal drivers, Atmos. Environ., 68, 208-220, doi:10.1016/j.atmosenv.2012.11.017, 2013.

Gosselin, M. I., Rathnayake, C. M., Crawford, I., Pöhlker, C., Fröhlich-Nowoisky, J., Schmer, B., Després, V. R., Engling, G., Gallagher, M., Stone, E., Pöschl, U., and Huffman, J. A.: Fluorescent bioaerosol particle, molecular tracer, and fungal spore concentrations during dry and rainy periods in a semi-arid forest, Atmos. Chem. Phys., 16, 15165–15184, https://doi.org/10.5194/acp-16-15165-2016, 2016.

Healy, D. A., Huffman, J. A., O'Connor, D. J., Pöhlker, C., Pöschl, U., and Sodeau, J. R.: Ambient measurements of biological aerosol particles near Killarney, Ireland: a comparison between real-time fluorescence and microscopy techniques, Atmos. Chem. Phys., 14, 8055–8069, https://doi.org/10.5194/acp-14-8055-2014, 2014.

Hernandez, M., Perring, A. E., McCabe, K., Kok, G., Granger, G., and Baumgardner, D.: Chamber catalogues of optical and fluorescent signatures distinguish bioaerosol classes, Atmos. Meas. Tech., 9, 3283–3292, https://doi.org/10.5194/amt-9-3283-2016, 2016.

Ho, J., Spence, M., and Hairston, P.: Measurement of Biological Aerosol with a Fluorescent Aerodynamic Particle Sizer (FLAPS): Correlation of Optical Data with Biological Data, Aerobiologia, 15, 281, https://doi.org/10.1023/A:1007647522397, 1999.

Hoose, C., Kristjánsson, J. E. and Burrows, S. M.: How important is biological ice nucleation in clouds on a global scale?, Environ. Res. Lett., 5(2), 024009, doi:10.1088/1748-9326/5/2/024009, 2010.

Huffman, J. A. and Santarpia, J. L.: Online techniques for quantification and characterization of biological aerosol, in: Microbiology of Aerosols, edited by: Delort, A. M. and Amato, P., Wiley, Hoboken, NJ, chap. 1.4, 2017.

Jaenicke, R.: Abundance of cellular material and proteins in the atmosphere, Science (80-.)., 308(5718), 73. doi:10.1126/science.1106335, 2005.

Kaye, P. H., Stanley, W. R., Hirst, E., Foot, E. V., Baxter, K. L., and Barrington, S. J.: Single particle multichannel bio-aerosol fluorescence sensor, Opt. Express, 13, 3583-3593, 2005.

Kaye, P. H., Aptowicz, K., Chang, R. K., Foot, V., and Videen, G.: Angularly resolved elastic scattering from airborne particles - Potential for characterizing, classifying, and identifying individual aerosol particles, Opt. Biol. Part., 238, 31–61, 2007.

Kulkarni, P., Baron, P. A. and Willeke, K.: Aerosol Measurement: Principles, Techniques, and Applications: Third Edition., 2011.Möhler, O., DeMott, P. J., Vali, G., and Levin, Z.: Microbiology and atmospheric processes: the role of biological particles in cloud physics, Biogeosciences, 4, 1059–1071, doi:10.5194/bg-4-10592007, 2007.

Oliveira, M., Ribeiro, H. and Abreu, I.: Annual variation of fungal spores in atmosphere of Porto: 2003, Ann. Agric. Environ. Med., 12(2), 309-315, 2005.

Ortiz-Martínez, M. G., Rodríguez-Cotto, R. I., Ortiz-Rivera, M. A., Pluguez-Turull, C. W. and

Jiménez-Vélez, B. D.: Linking Endotoxins, African Dust PM_{10} and Asthma in an Urban and Rural Environment of Puerto Rico, Mediators Inflamm., 2015, 784212, doi:10.1155/2015/784212, 2015.

Perring, A. E., Schwarz, J. P., Baumgardner, D., Hernandez, M. T., Spracklen, D. V., Heald, C. L., Gao, R. S., Kok, G., McMeeking, G. R., McQuaid, J. B., and Fahey, D. W.: Airborne observations of regional variation in fluorescent aerosol across the United States, J. Geophys. Res.-Atmos., 120, 1153–1170, https://doi.org/10.1002/2014JD022495, 2015.

Pope, F. D.: Pollen grains are efficient cloud condensation nuclei, Environ. Res. Lett., 5, 044015, doi:10.1088/17489326/5/4/044015, 2010.

Quintero, E., Rivera-Mariani, F. and Bolaños-Rosero, B.: Analysis of environmental factors and their effects on fungal spores in the atmosphere of a tropical urban area (San Juan, Puerto Rico), Aerobiologia (Bologna)., 26, 113–124, doi:10.1007/s10453-009-9148-0, 2010.

Raga, G. B., Baumgardner, D. and Mayol-Bracero, O. L.: History of aerosol-cloud interactions derived from observations in mountaintop clouds in Puerto Rico, Aerosol Air Qual. Res., 16, 674–688, doi:10.4209/aaqr.2015.05.0359, 2016.

Roberts, G. C. and Nenes, A.: A Continuous-Flow Streamwise Thermal-Gradient CCN Chamber for Atmospheric Measurements, Aerosol Sci. Technol., 39, 206–221, 2005.

Rose, D., Gunthe, S. S., Mikhailov, E., Frank, G. P., Dusek, U., Andreae, M. O., and Pöschl, U.: Calibration and measurement uncertainties of a continuous-flow cloud condensation nuclei counter (DMT-CCNC): CCN activation of ammonium sulfate and sodium chloride aerosol particles in theory and experiment, Atmos. Chem. Phys., 8, 1153–1179, https://doi.org/10.5194/acp-8-1153-2008, 2008.

Rivera-Mariani, F. E., Nazario-Jiménez, S., López-Malpica, F. and Bolaños-Rosero, B.: Sensitization to airborne ascospores, basidiospores, and fungal fragments in allergic rhinitis and asthmatic subjects in San Juan, Puerto Rico, Int. Arch. Allergy Immunol., 155, 322-334, doi:10.1159/000321610, 2011.

Rivera-Mariani, F. E., Almaguer, M., Aira, M. J. and Bolaños-Rosero, B.: Comparison of atmospheric fungal spore concentrations between two main cities in the Caribbean basin, P. R. Health Sci. J., 39(3), 235–242, 2020.

Sarangi, B., Baumgardner, D., Bolaños-Rosero, B. and Mayol-Bracero, O. L.: Dataset to:

Measurement Report: An Exploratory Study of Fluorescence and CCN Activity of Urban Aerosols in San Juan, Puerto Rico, Mendeley Data, Version 1, doi:10.17632/t26dctfk7t.1, 2021.

Savage, N. J., Krentz, C. E., Könemann, T., Han, T. T., Mainelis, G., Pöhlker, C. and Alex Huffman, J.: Systematic characterization and fluorescence threshold strategies for the wideband integrated bioaerosol sensor (WIBS) using size-resolved biological and interfering particles, Atmos. Meas. Tech., 10, 4279–4302, doi:10.5194/amt-10-4279-2017, 2017.

Spiegel, J. K., Buchmann, N., Mayol-Bracero, O. L., Cuadra-Rodriguez, L. A., Valle Díaz, C. J., Prather, K. A., Mertes, S. and Eugster, W.: Do Cloud Properties in a Puerto Rican Tropical Montane Cloud Forest Depend on Occurrence of Long-Range Transported African Dust?, Pure Appl. Geophys., 171(9), 2443–2459, https://doi.org/10.1007/s00024-014-0830-y, 2014.

Stanley, W. R., Kaye, P. H., Foot, V. E., Barrington, S. J., Gallagher, M. and Gabey, A.: Continuous bioaerosol monitoring in a tropical environment using a UV fluorescence particle spectrometer, Atmos. Sci. Lett., 12, 195–199, doi:10.1002/asl.310, 2011.

Stocker, T.F., Qin, D., Plattner, G.-K., Tignor, M., Allen, S.K., Boschung, J., Nauels, A., Xia, Y., Bex, V., Midgley, P.M., 2013. IPCC, 2013: climate change 2013: the physical science basis. Contribution of working group I to the fifth assessment report of the intergovernmental panel on climate change. IPCC, 2013. Cambridge University Press, Cambridge, United Kingdom and New York, NY, USA, p. 1535. Stommel, E.W., Fiel

Stolzenburg, M. R. and McMurry, P. H.: An Ultrafine Aerosol Condensation Nucleus Counter, Aerosol Sci. Tech., 14, 48–65, 1991.

Toprak, E. and Schnaiter, M.: Fluorescent biological aerosol particles measured with the Waveband Integrated Bioaerosol Sensor WIBS-4: laboratory tests combined with a one year field study, Atmos. Chem. Phys., 13, 225–243, https://doi.org/10.5194/acp-13-225-2013, 2013.

Torres-Delgado, E., Baumgardner, D., and Mayol-Bracero, O. L.: Measurement Report: Impact of African Aerosol Particles on Cloud Evolution in a Tropical Montane Cloud Forest in the Caribbean, Atmos. Chem. Phys. Discuss. [preprint], https://doi.org/10.5194/acp-2021-88, in review, 2021.

Toro-Heredia, J., Jirau-Colón, H. and Jiménez-Vélez, B. D.: Linking PM2.5 organic constituents, relative toxicity and health effects in Puerto Rico, Environ. Challenges, 5, 100350, doi:10.1016/j.envc.2021.100350, 2021.

Twohy, C. H., McMeeking, G. R., DeMott, P. J., McCluskey, C. S., Hill, T. C. J., Burrows, S. M., Kulkarni, G. R., Tanarhte, M., Kafle, D. N., and Toohey, D. W.: Abundance of fluorescent biological aerosol particles at temperatures conducive to the formation of mixed-phase and cirrus clouds, Atmos. Chem. Phys., 16, 8205–8225, https://doi.org/10.5194/acp-16-8205-2016, 2016.

Valle-Díaz, C. J., Torres-Delgado, E., Colón-Santos, S. M., Lee, T., Collett, J. L., McDowell, W. H., & Mayol-Bracero, O. L.: Impact of long-range transported african dust on cloud water chemistry at a tropical montane cloud forest in Northeastern Puerto Rico. Aerosol and Air Quality Research, 16(3), 653–664. doi.org/10.4209/aaqr.2015.05.0320, 2016.

Velázquez-Lozada, A., Gonza´lez, J. E., and Winter, A.: Urban heat islands effect analysis for San Juan, Puerto Rico. Atmospheric Environment, 40, 1731–1741, 2006.

Uin, J.: Ultra-High Sensitivity Aerosol Spectrometer (UHSAS) instrument handbook. ARM Tech. Rep. DOE/SCARM-TR-163, USA, 17 pp., doi.org/10.2172/1251410, 2016.

Zhang, M., Khaled, A., Amato, P., Delort, A.-M., and Ervens, B.: Sensitivities to biological aerosol particle properties and ageing processes: potential implications for aerosol–cloud interactions and optical properties, Atmos. Chem. Phys., 21, 3699–3724, https://doi.org/10.5194/acp-21-3699-2021, 2021.